

Article

Not peer-reviewed version

Modeling and Prediction of Thermal Deformation Errors in Fiber Optic Gyroscopes Based on the TD-model

[Jintao Xu](#) , [Ailing Tian](#) ^{*} , [Hui Liu](#) , [Ying Liu](#)

Posted Date: 13 October 2023

doi: 10.20944/preprints202310.0871.v1

Keywords: fiber optic gyroscope; thermal errors; prediction model; overfitting; biased regression



Preprints.org is a free multidiscipline platform providing preprint service that is dedicated to making early versions of research outputs permanently available and citable. Preprints posted at Preprints.org appear in Web of Science, Crossref, Google Scholar, Scilit, Europe PMC.

Copyright: This is an open access article distributed under the Creative Commons Attribution License which permits unrestricted use, distribution, and reproduction in any medium, provided the original work is properly cited.

Article

Modeling and Prediction of Thermal Deformation Errors in Fiber Optic Gyroscopes Based on the TD-Model

Jintao Xu ^{1,2}, Ailing Tian ^{1,*}, Hui Liu ³ and Liu Ying ³

¹ Key Laboratory of Thin Film Technology and Optical Testing in Shaanxi Province, School of Opto-Electronic Engineering, Xi'an Technological University, Xi'an 710021, China; xujintao@opt.ac.cn

² Xi'an Zhongke Huaxin Measurement & Control Co., Ltd., Xi'an 710119, China

³ Xi'an University of Posts & Telecommunications, Xi'an 710121, China

* Correspondence: ailintian@xatu.edu.cn

Abstract: For a fiber optic gyroscope, thermal deformation of the fiber coil can introduce additional thermal-induced phase errors, commonly referred to as thermal errors. Thermal error compensation techniques are effective means of addressing this issue. The principle behind these techniques involves real-time sensing of thermal errors and correcting them within the output signal. Since it is challenging to directly separate thermal errors from the output signal of the fiber optic gyroscope, it is necessary to predict thermal errors based on temperature. To establish a mathematical model between temperature and thermal errors, this paper measured synchronized data of phase errors and angular velocity for the fiber coil under different temperature conditions and aimed to model it using data-driven methods. Due to the difficulty of conducting tests and the limited number of data samples, an algorithm called TD-model modeling is proposed to address the issue of overfitting, which can reduce the model's generalization ability. First, a theoretical analysis of the phase errors caused by thermal deformation of the fiber coil is performed. Subsequently, the critical parameters, such as the thermal expansion coefficient, are determined, and a theoretical model is established. Finally, the theoretical analysis model is incorporated as a regularization term and combined with the test data to jointly participate in the regression of model coefficients. Through experimental comparative analysis, it is shown that, relative to ordinary regression models, the TD-model effectively mitigates overfitting caused by the limited number of samples, leading to a 58% improvement in predictive accuracy.

Keywords: fiber optic gyroscope; thermal errors; prediction model; overfitting; biased regression

1. Introduction

The fiber optic gyroscope, based on the Sagnac effect, represents a new generation of high-performance inertial sensors. It has gained prominence as the preferred inertial instrument for medium and high-precision inertial navigation systems due to its outstanding advantages such as high accuracy, solid-state design, and high reliability. It finds extensive applications in various domains, including marine, terrestrial, aerial, and space sectors [1, 2]. Currently, there are two primary technical approaches for fiber optic gyroscopes: the traditional fiber optic gyroscope with discrete packaging of core optical components and the integrated optical fiber gyroscope. With the rapid development of optoelectronics, microelectronics, and micro/nano-processing technologies, integrated optical chips that combine various functions such as emission, coupling, modulation, and detection have made significant breakthroughs. These integrated optical chips are widely used in the field of optical communications, especially silicon-based photonic devices that are compatible with traditional CMOS processes. They offer advantages like compact size, high performance, and cost-effectiveness, making them a key technological solution for future photonic integration [3,4]. Whether it is the traditional discrete fiber optic gyroscope or the integrated optical fiber gyroscope, the optical fiber coil serves as the sensitive core component, and its performance directly impacts the engineering precision of fiber optic gyroscopes [5].

The temperature performance of the optical fiber coil has the most significant impact on the zero bias error of the fiber optic gyroscope [6]. When the fiber optic gyroscope is used in high-temperature environments, temperature effects can cause geometric deformation of the optical fiber coil, deviating from its original output characteristics, resulting in thermal errors. For sensing devices whose working principles depend on geometric characteristics, thermal errors are an unavoidable source of error [7,8]. Currently, thermal error compensation is an effective means to reduce thermal deformation errors. It calculates the thermal error magnitude at various temperatures through algorithms and provides feedback compensation. Its advantage lies in not requiring hardware modifications; it can reduce thermal errors through software alone [9]. The key to thermal error compensation is the ability to obtain accurate thermal error values. However, for fiber optic gyroscopes, thermal errors are difficult to directly separate from the measured values. Therefore, it is feasible to indirectly predict thermal errors based on temperature. However, this approach requires the establishment of a mathematical model between thermal errors and temperature for the fiber optic gyroscope. In theory, if the thermal expansion coefficient of the optical fiber coil is known, it is possible to derive the additional phase error caused by temperature based on its working principle. However, the material composition of fiber optic gyroscopes is complex, including not only the core but also cladding, stress zones, inner coatings, and outer layers [10]. This complexity makes it difficult to determine the comprehensive thermal expansion coefficient when various materials are combined. Additionally, due to differences in manufacturing processes for different fiber optic gyroscopes and variations between production batches, it is challenging to establish a quantitative thermal error model for fiber optic gyroscopes purely through theoretical derivation.

In addition to pure theoretical derivation, data-driven methods are also an effective approach for modeling complex objects. For thermal deformation errors in fiber optic gyroscopes, it is possible to directly measure phase errors at different temperatures and model them based on data. This method has been widely applied in the study of thermal errors in numerical control machine tools [11], with the common practice being the establishment of a model between key points' temperatures on the machine tool and thermal errors. Multiple regression benefits from its simplicity and fast computation speed, making it the most commonly used method. Mayr [12] and Zimmermann [13,14] utilized multiple regression algorithms to propose a thermal error compensation mechanism that updates the model online. It assesses the model's effectiveness through periodic accuracy checks, supplements new measurement data if the model becomes ineffective, and rebuilds the model. Wei [15], using the Gaussian process regression algorithm, established an adaptive thermal error model that adjusts according to environmental changes. Machine tool structures vary widely, and some exhibit complex thermal deformation error patterns. Therefore, neural networks have also found extensive application. Li [16] combined stochastic theory, genetic algorithms, and the radial basis function neural network (RBFNN) algorithm to create a comprehensive model that considers thermal errors, temperature, and random disturbance factors, thereby improving the robustness of thermal error prediction. Liu [17,18] leveraged the long-term memory properties of LSTM neural networks to establish thermal error models, allowing multiple time data points to contribute to thermal error prediction and enhancing prediction accuracy. Additionally, some researchers [19] have based their work on convolutional neural networks, using deep learning to directly establish mathematical models between the overall machine tool temperature field and thermal errors.

In the aforementioned research on modeling thermal errors in numerical control machine tools, despite using different algorithms, they all employed the same fundamental strategy: increasing the number of modeling samples to enhance the model's generalization properties and reduce overfitting. Overfitting [20] can lead the model to fit irrelevant information from the training data, such as errors, leading to a significant deterioration in the model's predictive performance on data not included in the modeling process. The scarcity of modeling data samples is one of the reasons for the overfitting problem, and it is also a central challenge in modeling thermal deformation errors in fiber optic gyroscopes. Modeling thermal deformation errors in fiber optic gyroscopes is challenging because the measurement of these errors is difficult. Each temperature point measurement requires a relatively long wait time to allow the temperature field to reach equilibrium. For mass-produced

products, it is challenging to perform intensive temperature interval sampling. Additionally, the performance of sensors can be highly unstable under frequent temperature fluctuations, necessitating frequent compensation and correction of the sensor's own thermal errors. All these factors lead to data-driven modeling of thermal deformation errors in fiber-optic gyroscopes, and it is necessary to overcome the overfitting problem caused by a small sample size.

In response to these challenges, this paper introduces a modeling algorithm that combines theoretical models with modeling data. Taking into account the stability of the fiber optic gyroscope's material, it is possible to deduce the comprehensive thermal expansion coefficient of the optical fiber material and establish a theoretical model for thermal deformation errors in the fiber optic gyroscope through a single intensive temperature experiment. Subsequently, for different batches of fiber optic gyroscopes, while there may be process variations, the resulting characteristic changes can be distributed around the theoretical model following a certain probability density function. If a confidence probability is set, and it is believed that the occurrence of characteristics outside the confidence probability is a rare event, then the distribution of characteristic variations remains within a limited range around the theoretical model. This indicates that the theoretical model still contains valuable information. Consequently, when modeling, the theoretical model can be used as a regularization term, combined with small-sample data to address overfitting issues. Based on this, the algorithm proposed in this paper is referred to as the TD-model modeling algorithm, and its effectiveness is validated through experiments. Based on this approach, the algorithm proposed in this paper is referred to as the TD-model modeling algorithm, and its effectiveness has been experimentally validated.

2. The Principle of a Fiber Optic Gyroscope

Figure 1 shows two beams of light, A and B, propagating along a fiber optic ring in different directions. In this setup, fiber optic A travels through the fiber optic ring in a clockwise direction, while fiber optic B travels in a counterclockwise direction. Both fiber optic beams follow a path with a radius of R within the fiber optic ring.

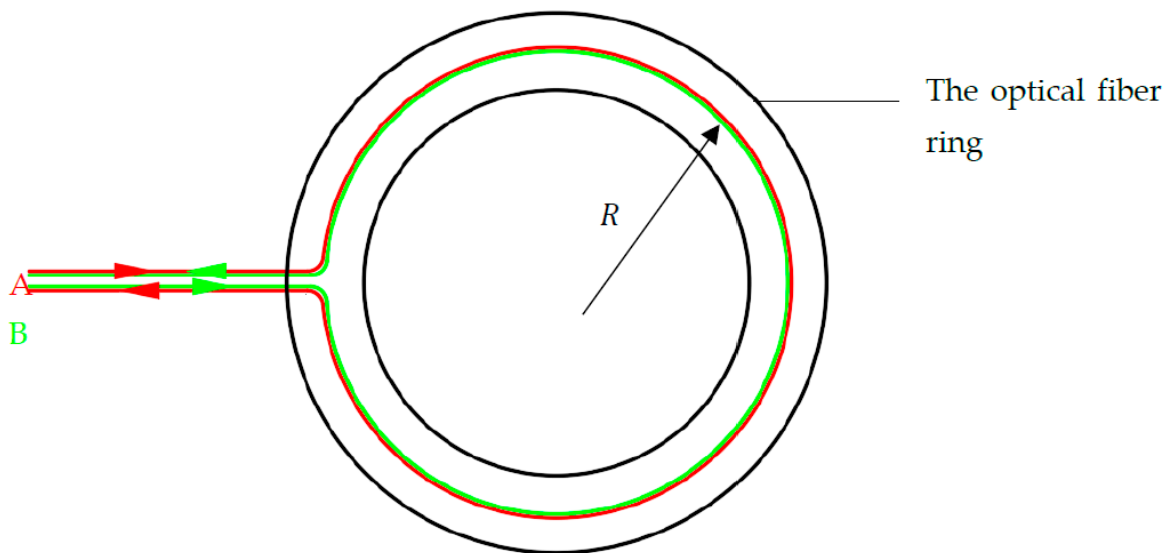


Figure 1. Fiber optic coil (Stationary state).

The geometric distance traveled by two optical fibers within a stationary optical fiber ring is equal, as follows.

$$L_A^0 = L_B^0 = 2\pi R \quad (1)$$

Now, if the optical fiber ring rotates at a certain angular velocity Ω , such as clockwise as shown in Figure 2.

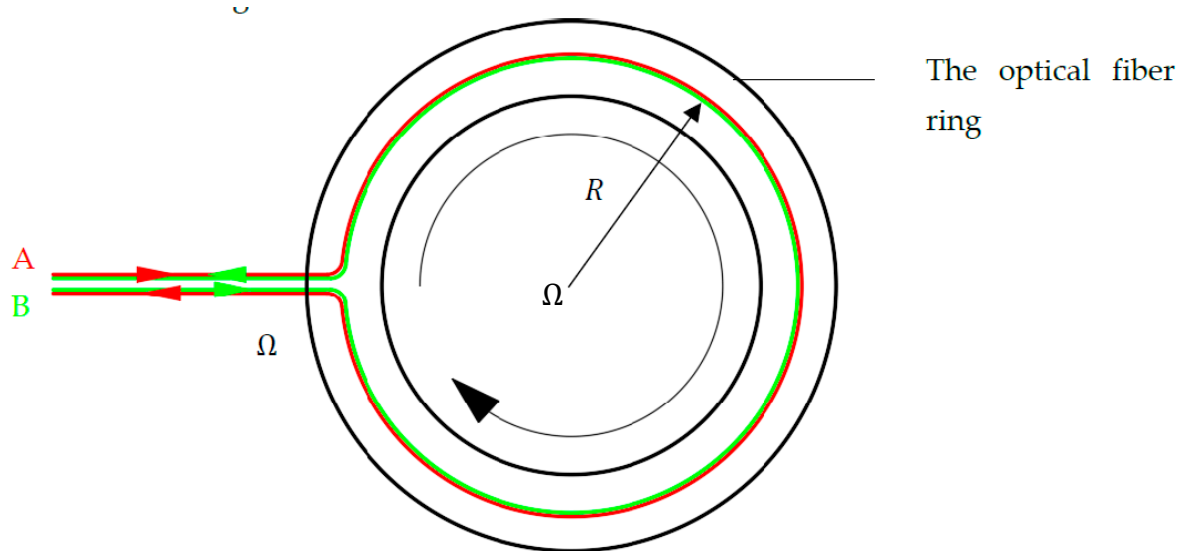


Figure 2. Optical fiber ring (Rotational state).

According to the Sagnac effect, the geometric distance traveled by light beams A and B around the optical fiber ring is no longer equal, as follows.

$$\begin{cases} L_A = 2\pi R + R\Omega t_A \\ L_B = 2\pi R - R\Omega t_B \end{cases} \quad (2)$$

In which, L_A and L_B represent the geometric distances traveled by light beams A and B around the optical fiber ring for one complete rotation, and t_A and t_B denote the time spent.

Therefore, when the optical fiber ring starts to rotate, there is a certain optical path difference between the two light beams at the exit position, resulting in a phase difference $\Delta\Phi$. By measuring the phase difference $\Delta\Phi$ between the two light beams, the rotational angular velocity Ω of the optical fiber ring can be calculated.

According to the Lorentz-Einstein velocity transformation formula, the propagation velocities of light beams A and B in the rotating optical fiber ring no longer have a simple proportionality relationship with the refractive index. Specifically, as follows.

$$\begin{cases} c_A = \frac{c_0/n + R\Omega}{1 + R\Omega/(nc_0)} \\ c_B = \frac{c_0/n - R\Omega}{1 - R\Omega/(nc_0)} \end{cases} \quad (3)$$

Where c_A and c_B are the propagation velocities of light beams A and B within the optical fiber ring, c_0 is the speed of light in a vacuum, and n is the refractive index of the optical fiber ring.

Combining equations (2) and (3), it can be seen that...

$$\begin{cases} t_A = \frac{L_A}{c_A} = \frac{(2\pi R + R\Omega t_A)(1 + R\Omega/(nc_0))}{c_0/n + R\Omega} \\ t_B = \frac{L_B}{c_B} = \frac{(2\pi R - R\Omega t_B)(1 - R\Omega/(nc_0))}{c_0/n - R\Omega} \end{cases} \quad (4)$$

$$\Rightarrow \begin{cases} t_A = \frac{2\pi R(nc_0 + R\Omega)}{c_0^2 - (R\Omega)^2} \\ t_B = \frac{2\pi R(nc_0 - R\Omega)}{c_0^2 - (R\Omega)^2} \end{cases} \quad (5)$$

Because the frequency of light remains constant while propagating through a medium, therefore...

$$f = \frac{c_A}{\lambda_A} = \frac{c_B}{\lambda_B} = \frac{c_0}{\lambda_0} \quad (6)$$

Where λ_A , λ_B , and λ_0 represent the wavelengths of light beams A, B, and in vacuum, respectively.

Furthermore, it is possible to calculate the number of wavelengths experienced by light beams A and B after one rotation around the optical fiber ring, denoted as k_A and k_B , respectively. As follows:

$$\begin{cases} k_A = \frac{c_A}{\lambda_A} t_A = \frac{c_0}{\lambda_0} t_A \\ k_B = \frac{c_B}{\lambda_B} t_B = \frac{c_0}{\lambda_0} t_B \end{cases} \quad (7)$$

Subsequently, when light beams A and B converge, the difference in the number of wavelengths between them is...

$$\Delta k = (k_A - k_B) = (t_A - t_B) \frac{c_0}{\lambda_0} = \frac{4\pi R^2}{c_0^2 - (R\Omega)^2} \Omega \frac{c_0}{\lambda_0} \quad (8)$$

Due to

$$c_0 \gg R\Omega \quad (9)$$

Equation (8) can be simplified to...

$$\Delta k = \frac{4\pi R^2}{c_0^2} \Omega \frac{c_0}{\lambda_0} = \frac{4\pi R^2}{c_0 \lambda_0} \Omega \quad (10)$$

Therefore, the phase difference is...

$$\Delta\Phi = 2\pi\Delta k = 2\pi^2 \frac{D^2}{c_0 \lambda_0} \Omega \quad (11)$$

For an N-turn optical fiber, every turn generates a phase difference $\Delta\Phi$, and consequently, the total phase difference for an N-turn optical fiber ring is...

$$\Delta\Phi = 2\pi N \Delta k = 2\pi^2 N \frac{D^2}{c_0 \lambda_0} \Omega \quad (12)$$

3. The Thermal Error Model for a Fiber Optic Gyroscope

From a fundamental analysis, derive the theoretical model of thermal errors in optical fibers under conditions of uniform temperature variation. Through extensive experimental regression, obtain the key parameters to provide theoretical support for modeling mass-produced products, addressing overfitting issues arising from modeling with small-scale data, and reducing the dependency on data for subsequent mass-produced product modeling.

3.1. The theoretical form of the thermal error model

According to equation (12), when the optical fiber ring is subjected to heating, its diameter changes, leading to a variation in the proportionality factor between the phase difference $\Delta\Phi$ and the angular velocity Ω (denoted as $K_{\Delta\Phi/\Omega}$). Assuming the function describing the change in optical fiber ring diameter with temperature is $D(\Delta t)$, then...

$$K_{\Delta\Phi/\Omega}(\Delta t) = 2\pi^2 N \frac{D(\Delta t)^2}{c_0 \lambda_0} \quad (13)$$

Where the parameters c_0, λ_0 and N are all known values. The key to the model lies in $D(\Delta t)$. For a circular ring made of a single material, it follows that...

$$D(\Delta t) = D_0 + \alpha D_0 \Delta t \quad (14)$$

Substituting equations (13) and (14) into equation (12), we obtain...

$$\Delta\Phi(\Delta t) = \frac{2N(\pi D_0 \alpha)^2}{c_0 \lambda_0} \Delta t^2 \Omega + \frac{4ND_0 \alpha (\pi)^2}{c_0 \lambda_0} \Delta t \Omega + \frac{2N(\pi D_0)^2}{c_0 \lambda_0} \Omega \quad (15)$$

Where α is the coefficient of thermal expansion, and D_0 is the diameter of the optical fiber ring when $\Delta t = 0$, for example, if taken as a reference at 20°C, then D_0 is the diameter at 20°C. However, equation (15) is difficult to apply to the actual structure of the optical fiber ring because its interior is composed of multiple materials, making it challenging to determine the comprehensive coefficient of thermal expansion after the composite of various materials.

3.2. Method for determining the comprehensive coefficient of thermal expansion in the thermal error model

Selecting a specific optical fiber ring, conducting a large-scale experiment, and regressing experimental data to obtain the value of the comprehensive coefficient of thermal expansion, denoted as α^* . Substituting α^* into equation (15), we can derive...

$$\Delta\Phi(\Delta t) = \frac{2N(\pi D_0 \alpha^*)^2}{c_0 \lambda_0} \Delta t^2 \Omega + \frac{4ND_0 \alpha^* (\pi)^2}{c_0 \lambda_0} \Delta t \Omega + \frac{2N(\pi D_0)^2}{c_0 \lambda_0} \Omega \quad (16)$$

Subsequently, we can establish the following model form...

$$y = k_2 x_2 + k_1 x_1 + k_0 \quad (17)$$

Where,

$$\begin{cases} x_1 = \Delta t \\ x_2 = \Delta t^2 \\ y = \frac{\Delta\Phi}{\Omega} \end{cases} \quad (18)$$

According to equation (18), it is possible to measure the phase difference of the optical fiber ring at different temperatures and different rotational speeds, calculate the measured values of x_1, x_2 and y , and then perform regression to obtain the values of k_0, k_1 , and k_2 . According to equation (16), it is evident that by utilizing k_0, k_1 , and k_2 separately, it is possible to estimate α^* , as follows...

$$\begin{cases} \alpha^*_{m1} = \sqrt{\frac{k_2 c_0 \lambda_0}{2N(\pi D_0)^2}} \\ \alpha^*_{m2} = \frac{k_1 c_0 \lambda_0}{4N(\pi)^2 D_0} \\ \alpha^*_{m3} = \sqrt{\frac{k_2}{k_0}} \end{cases} \quad (19)$$

To obtain an accurate estimate of α^* , it is possible to assess the precision of the three methods separately. First, assess the estimation precision of k_0, k_1 , and k_2 , as follows...

$$\begin{pmatrix} \sigma_{k_0} \\ \sigma_{k_1} \\ \sigma_{k_2} \end{pmatrix} = \sigma \begin{pmatrix} \sqrt{d_{11}} \\ \sqrt{d_{22}} \\ \sqrt{d_{33}} \end{pmatrix} \quad (20)$$

Where,

$$\text{diag}((A^T A)^{-1}) = \begin{pmatrix} d_{11} & & \\ & d_{22} & \\ & & d_{33} \end{pmatrix} \quad (21)$$

$$A = \begin{pmatrix} x_{11} & x_{21} \\ \vdots & \vdots \\ x_{1n} & x_{2n} \end{pmatrix} \quad (22)$$

$$\sigma = \sqrt{\frac{\sum_{j=1}^n v_j^2}{n-2}} \quad (23)$$

$$v_j = y_j - \hat{y}_j = k_2 x_{2j} + k_1 x_{1j} + k_0 \quad (24)$$

Where, x_{i1}, \dots, x_{in} are n measured values of variable x_i , and v_1, \dots, v_n are the estimated residuals when the n measurements are plugged into the model. Ultimately, ...

$$\alpha^* = \frac{(\sigma_{\alpha^*_{m2}} + \sigma_{\alpha^*_{m3}}) \alpha^*_{m1} + (\sigma_{\alpha^*_{m1}} + \sigma_{\alpha^*_{m3}}) \alpha^*_{m2} + (\sigma_{\alpha^*_{m1}} + \sigma_{\alpha^*_{m2}}) \alpha^*_{m3}}{\sigma_{\alpha^*_{m1}} + \sigma_{\alpha^*_{m2}} + \sigma_{\alpha^*_{m3}}} \quad (25)$$

Where $\sigma_{\alpha^*_{m1}}, \sigma_{\alpha^*_{m2}}$ and $\sigma_{\alpha^*_{m3}}$ represent the estimated standard deviations for the three methods, which can be calculated using the uncertainty synthesis formula based on $\begin{pmatrix} \sigma_{k_0} \\ \sigma_{k_1} \\ \sigma_{k_2} \end{pmatrix}$ and equation (19), as shown in equation (25).

$$\begin{cases} \sigma_{\alpha^*_{m1}} = \sqrt{\left(\frac{\partial \alpha^*_{m1}}{\partial k_2} \sigma_{k_2}\right)^2 + \left(\frac{\partial \alpha^*_{m1}}{\partial D_0} \sigma_{D_0}\right)^2} \\ \sigma_{\alpha^*_{m2}} = \sqrt{\left(\frac{\partial \alpha^*_{m2}}{\partial k_1} \sigma_{k_1}\right)^2 + \left(\frac{\partial \alpha^*_{m2}}{\partial D_0} \sigma_{D_0}\right)^2} \\ \sigma_{\alpha^*_{m3}} = \sqrt{\left(\frac{\partial \alpha^*_{m3}}{\partial k_0} \sigma_{k_0}\right)^2 + \left(\frac{\partial \alpha^*_{m3}}{\partial k_2} \sigma_{k_2}\right)^2} \end{cases} \quad (26)$$

Where, $\sigma_{(D_0)}$ represents the standard deviation of the optical fiber ring diameter measurements.

3.3. Method for establishing the thermal error model

For subsequent mass-produced optical fiber rings, the thermal error model has the form of equations (16) and (17). After obtaining the value of α^* , even if its number of turns and inner diameter change, as long as the internal material remains unchanged, it is possible to calculate the theoretical values of k_0, k_1 , and k_2 in the corresponding thermal error model of the optical fiber ring. However, considering the process differences, each optical fiber ring still needs to undergo thermal error testing experiments to establish a high-precision thermal error model based on data.

However, during the model-building process, it is possible to effectively integrate the theoretical values of k_0, k_1 , and k_2 with the testing data, reducing the dependency of model construction on the quantity of testing data samples. The specific method involves adding the theoretical values of k_0, k_1 , and k_2 as regularization terms to the objective function of the regression algorithm when performing regression on testing data, as shown in equation (27).

$$\min_{k_0, k_1, k_2} \Gamma = ((1 - \eta) \sum_{j=1}^n v_j^2 + \eta \sum_{i=0}^2 (k_i - k_i^*)^2) \quad (27)$$

Where k_i^* represents the theoretical value of k_i , and $\eta=[0,1]$ is the weight of the regularization term. This algorithm is actually an extension of ridge regression. If k_i^* is set to 0, equation (27) becomes ridge regression. Therefore, with a small weight for the regularization term, it can significantly reduce the estimation error of model coefficients. In this study, $\eta=0.1$ was chosen. The solution method is as shown in equation (28).

$$\begin{cases} \frac{\partial \Gamma}{\partial k_0} = 0 \\ \vdots \\ \frac{\partial \Gamma}{\partial k_2} = 0 \end{cases} \Rightarrow \begin{pmatrix} k_0 \\ k_1 \\ k_2 \end{pmatrix} = ((1 - \eta) \mathbf{A}^T \mathbf{A} + \eta \mathbf{I})^{-1} ((1 - \eta) \mathbf{A}^T \mathbf{Y} + \eta \mathbf{K}^*) \quad (28)$$

Where \mathbf{I} is the identity matrix, $\mathbf{Y} = (y_1, \dots, y_n)^T$ represents the testing data for variable y , and $\mathbf{K}^* = (k_0^*, k_1^*, k_2^*)^T$.

4. Verification Experiment

To validate the effectiveness of the fiber optic gyroscope's thermal error model, temperature variation experiments were conducted on the fiber optic gyroscope for detection.

4.1. Experimental plan

The optical fiber gyro was placed in a high-low temperature chamber, and the optical fiber phase variation was measured within the temperature range of -18 to 65°C and the angular velocity range of -860 to 860°/h. The experimental setup, as shown in Figure 3, involved mounting the gyroscope under test inside a temperature-controlled chamber with a rotating platform. The temperature was gradually reduced to -18°C at a rate of 2°C/min, followed by a 2-hour insulation period. The rotating platform was then tested at different speeds: $\pm 860, \pm 500, \pm 360, \pm 180, \pm 90, \pm 30, \pm 10, \pm 1, \pm 0.5, \pm 0.3$, and $\pm 0.1^\circ/\text{h}$, and so on, at 0°C, 25°C, 40°C, and 65°C, replicating the same tests at each temperature point.

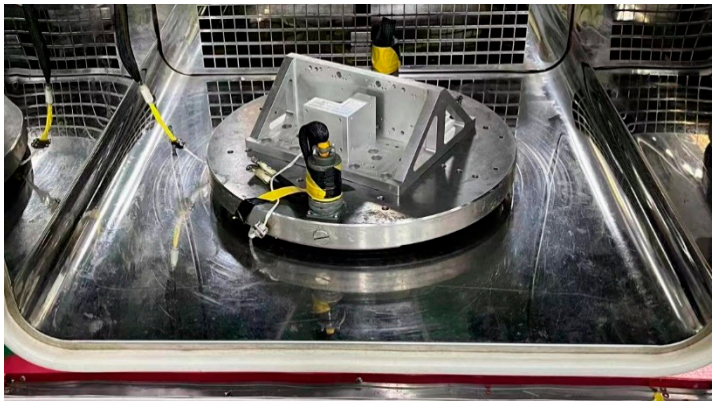


Figure 3. Experimental setup for thermal deformation error testing of fiber optic gyroscope.

Table 1. Experimental parameters for thermal deformation error testing of fiber optic gyroscope.

Temperature Test Points (°C)	Angular Velocity Test Points (°/h)	Fiber Optic Ring Parameters			
-18、0、25、40、65	±860、±500、±360、±180、±90、±30、±10、±1、±0.5、±0.3、±0.1	Diameter (mm)	winding method	number of layers	wavelength (nm)
		45.6	四极	20	650nm

4.2. Experimental data

As shown in Figure 4, these are the phase errors of the fiber optic gyroscope at each temperature test point.

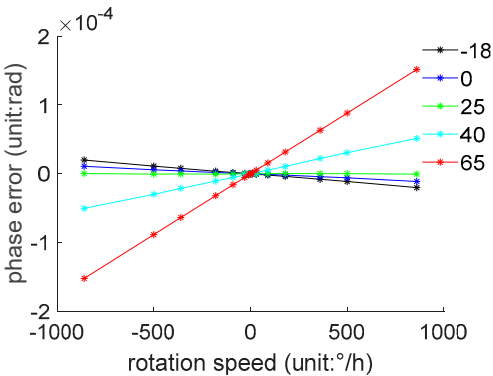


Figure 4. Experimental Data for Fiber Optic Gyroscope Thermal Deformation Error Testing.

For better visualization, the raw data in this study has been processed. Figure 4 represents the difference between the phase measurement values at each test point and the theoretical values under ideal conditions at 20°C. These differences are referred to as phase errors. The theoretical values are calculated by substituting the angular velocity values into equation (12).

It can be observed that as the temperature gradually increases, the phase error exhibits clear non-linearity but maintains a monotonous changing trend. The slope of the phase error with respect to angular velocity changes from negative values to positive values gradually, and with the rise in temperature, the rate of increase also becomes greater.

4.3. Experimental Results

To validate the effectiveness of the thermal error modeling, this study chose to build the model using data from three temperature test points: 0°C, 25°C, and 40°C. Subsequently, the data from two temperature test points, -18°C and 65°C, were used for prediction, serving as a test of the model's predictive accuracy for data not included in the modeling process.

First, based on equation (25), the comprehensive coefficient of thermal expansion for the optical fiber ring was estimated to be 0.76×10^{-5} . This value was then used in equation (16) to calculate the model's theoretical values. Subsequently, the theoretical values and measurement data were jointly used in equation (28) to establish the model, referred to as the Theoretical-Data-Driven model or TD-model. For the purpose of comparison, this study directly performed regression on the measurement data to establish a control model, known as the Pure Data model or OD-model.

Subsequently, based on the original measurement data, the input values required for the model predictions, namely $\Delta t^2\Omega$, $\Delta t\Omega$ and Ω as in equation (16), were computed. These values were separately used in the TD-model and OD-model to obtain model predictions, which were then compared with the actual measurement values, as shown in Figure 5.

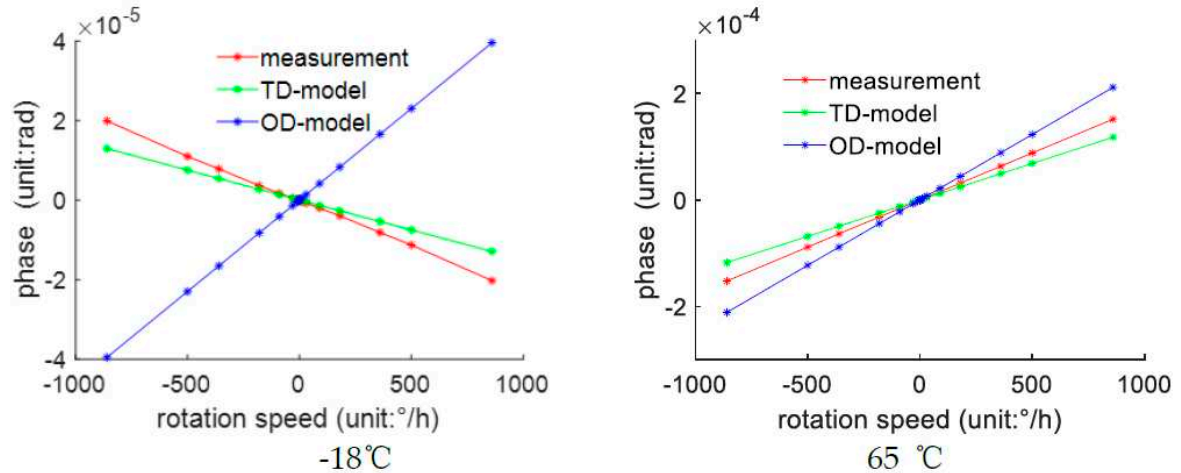


Figure 5. Comparison of Predictive Performance of the Fiber Optic Gyroscope Thermal Deformation Error Model.

It can be observed that the TD-model significantly outperforms the OD-model, especially in the -18°C environment where the OD-model exhibits predictive results that are completely opposite to the measurement values.

To quantitatively assess the predictive performance of the two modeling approaches, the relative root mean square error (RMSE) for each model's predictions of the measurement data was calculated. The RMSE calculation method is as shown in equation (29).

$$RMSE = \sqrt{\frac{\sum_{k=1}^n (y_k - \hat{y}_k)^2}{n}} \tag{29}$$

Where \hat{y}_k represents the model's prediction, and y_k represents the measured result. According to equation (11), RMSE reflects the sum of squares of differences between the model's predicted results and the actual measurement results. The larger the differences, the larger the RMSE. Using the range of measured values as the range, the relative RMSE as a percentage of the full-scale range was calculated, as shown in Table 2.

Table 2. Relative RMSE for Predictions of Fiber Optic Gyroscope Thermal Deformation Error Model.

TD-model	OD-model
3.0716%	7.3777%

The data indicates that the predictive accuracy of the TD-model is improved by 58% compared to the OD-model, demonstrating the effectiveness of the proposed algorithm.

5. Discussion

Discussing and analyzing the experimental results.

One of the most significant controversies encountered during the research process is why the predictive results of the OD-model at -18°C are opposite to the actual measurement values, while the TD-model provides accurate results.

The modeling data used for this study comes from measurements taken at temperatures of 0°C , 25°C , and 40°C . As observed in Figure 4, examining the variation in phase errors at these three temperature points reveals that if we fix the gyroscope at a certain rotational speed, the phase error decreases non-linearly and monotonically with respect to temperature. For example, at a rotational speed of $860^{\circ}/\text{h}$, plotting the variation curve of phase error with temperature and fitting it with a quadratic model results in the pattern shown in Figure 6.

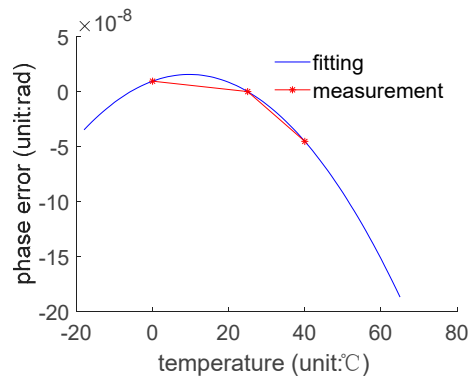


Figure 6. Observation of Measurement Data and Fitting for Phase Error vs. Temperature ($860^{\circ}/\text{h}$, 0°C , 25°C , 40°C).

It can be observed that although the measurement data exhibits a monotonically decreasing trend, the fitting results suggest that the most appropriate quadratic curve assumes that the phase error is monotonically increasing with temperature near 0°C , thereby leading to an overfitting issue. For other angular velocities, the same conclusion can be drawn, and thus, further elaboration is not necessary.

This issue is one of the reasons for introducing the TD-model. Fiber optic gyroscope testing experiments are relatively complex, making it difficult to conduct a large number of experiments, resulting in limited data. This limited data can easily lead to overfitting. The TD-model introduces a theoretical model to correct the distortion caused by overfitting. By observing equation (28), it can be seen that the TD-model's calculation formula is actually a variant of ridge regression [22]. If K^* is set to 0, it becomes ridge regression. According to the properties of ridge regression [23], a slight increase in the value of η , although causing a slight deviation of the model's expectation from the true value, leading from an unbiased regression to a biased regression, can effectively suppress overfitting. This significantly increases the probability of the model falling close to the true value. One difference between the TD-model and ridge regression is that if ridge regression increases the value of η , the model coefficients tend to approach zero, whereas the TD-model makes the model coefficients tend to be closer to the theoretical values of the true values. Thus, while suppressing overfitting, the TD-model significantly reduces the degree to which the model's expectation deviates from the true value, allowing for the establishment of a more effective model.

6. Conclusion

This paper has conducted modeling and analysis of the thermal deformation error in fiber optic gyroscopes. By combining theoretical derivation with experimental data, a new thermal error modeling algorithm has been proposed, significantly improving the modeling accuracy of thermal deformation error in fiber optic gyroscopes. The specifics are as follows.

1) Based on the working principles of fiber optic gyroscopes, a theoretical model was derived for the phase error induced by thermal deformation in the fiber optic ring, and its relationship with temperature and angular velocity. The model reveals that the phase error in fiber optic gyroscopes is quadratically related to temperature. However, obtaining a quantitative theoretical model relies on

accurate thermal expansion coefficients of the materials used in the fiber optic ring. Since the fiber optic ring is composed of multiple materials in combination, determining the thermal expansion coefficients theoretically becomes challenging.

Thermal deformation error measurement experiments were conducted on a specific model of fiber optic ring. Phase errors relative to the ideal environment at 20°C were measured at different angular velocities and temperatures. The experimental results revealed a nonlinear correlation between phase error and temperature, aligning with theoretical expectations. However, due to the complexity of the experiments and the difficulty in conducting them on a large scale, direct modeling using experimental data resulted in overfitting issues and poor predictive accuracy of the model. This paper introduces a novel modeling algorithm that combines the theoretically derived model with experimental data, effectively mitigating the overfitting problem. The model established is referred to as the Theory-Data Driven model, abbreviated as TD-model. It has been validated that the TD-model significantly enhances the predictive accuracy of phase errors induced by thermal deformation in fiber optic gyroscopes. Compared to a model based solely on experimental data, the TD-model demonstrates a 58% improvement in predictive accuracy, thus confirming the model's effectiveness.

Author Contributions: Conceptualization, J.X. and A.T.; methodology, J.X. and A.T.; software, J.X. and H.L.; validation, J.X. and A.T.; formal analysis, J.X. and A.T.; investigation, J.X. and Y.L.; resources, J.X.; data curation, J.X. and H.L.; writing—original draft preparation, J.X.; writing—review and editing, J.X.; visualization, J.X. and Y.L.; supervision, J.X. and A.T.; project administration, J.X. and A.T.; funding acquisition, J.X. All authors have read and agreed to the published version of the manuscript.

Funding: Please add: This research was funded by the National Natural Science Foundation of China, grant number: 52105274; This research was funded by Key Industry Chain Technology Research Project of Xi'an Municipal Science and Technology Bureau for 2023, grant number 23ZDCYJSGG0020-2023.

Institutional Review Board Statement: Not applicable.

Informed Consent Statement: Not applicable.

Data Availability Statement: The data underlying the results presented in this paper are not publicly available at this time but may be obtained from the authors upon reasonable request.

Conflicts of Interest: The authors declare no conflicts of interest.

References

1. SHANG Kejun, LEI Ming, LI Haowei, et al. Design, manufacturing and future development of the integrated fiber optic gyroscope. *Journal of Chinese Inertial Technology*, 2021, 29, pp. 502-509.
2. MAO Yuzheng, HE Jian, XIE Lianping, et al. Silicon photonics integrated chip based optical fiber gyroscope. *Journal of Chinese Inertial Technology*, 2023, 31, pp. 202-210.
3. Ryan B J, Diroll B T, Guo Y, et al. Silicon nanosheets as candidates for silicon-based optoelectronics. *ECS Trans.* 2021, 102, pp. 3-17.
4. LEI Ming, LI Haowei, YU Xiaozhi, et al. Development Status and Trend of integrated Fiber Optic Gyroscope. *SEMICONDUCTOR OPTOELECTRONICS*, 43, pp. 666-671.
5. Fan Yunqiang, Huang Jixun, Li JING. Temperature Performance Evaluation of Fiber Coil with Equivalent Asymmetric Length. *ACTA OPTICA SINICA*, 2306002.
6. Cao Y, Xu W, Lin B, et al. A method for temperature error compensation in fiber-optic gyroscope based on machine learning. *Optik*, 2022, 256, 168765.
7. Bryan, J. B. International Status of Thermal Error Research. *CIRP Annals* 1990, 39.
8. Aronson, R. B. War against thermal expansion. *Manufacturing Engineering* 1996, 116, pp. 45-50.
9. Gurauskis D, Kilikevičius A, Kasparaitis A. Thermal and geometric error compensation approach for an optical linear encoder. *Sensors*, 2021, 21, pp. 360.
10. LI Fenfei, Zhou Xiaoyan, Zhang KuiBao, et al. Effects of neutron irradiation on optical characteristics of Yb-doped fiber materials. *Acta Phys.Sin.*, 70, 190201.
11. Yang, L.; Zhao, W.; Lan, J S.; Ni, J.; Wu, W.; Lu, B. A review on spindle thermal error compensation in machine tools. *International Journal of Machine Tools and Manufacture* 2015, 95, pp. 20-38.

12. Mayr, J.; Blasér, P.; Ryser, A.; Hernandez-Becerroa, P. An adaptive self-learning compensation approach for thermal errors on 5-axis machine tools handling an arbitrary set of sample rates. *CIRP Annals* 2018, 67, pp. 551–554.
13. Zimmermann, N.; Lang, S.; Blaser, P.; Mayr, J. Adaptive input selection for thermal error compensation models. *CIRP Annals* 2020, 69, pp. 485–488.
14. Zimmermann, N.; Breu, M.; Mayr, J.; Wegener, K. Autonomously triggered model updates for self-learning thermal error compensation. *CIRP Annals* 2021, 70, pp. 431–434.
15. Wei X, Ye H, Miao E, et al. Thermal error modeling and compensation based on Gaussian process regression for CNC machine tools. *Precision Engineering*, 2022, 77, pp. 65-76.
16. Li T, Sun T, Zhang Y. Prediction of thermal error for feed system of machine tools based on random radial basis function neural network. *The International Journal of Advanced Manufacturing Technology*, 2021, 114, pp. 1545-1553.
17. Liu Y C, Li K Y, Tsai Y C. Spindle thermal error prediction based on LSTM deep learning for a CNC machine tool. *Applied Sciences*, 2021, 11(12): 5444.
18. Liu J, Ma C, Gui H, et al. Thermally-induced error compensation of spindle system based on long short term memory neural networks. *Applied Soft Computing*, 2021, 102, 107094.
19. Chengyang W, Sitong X, Wansheng X. Thermal error modeling of rotary axis based on convolutional neural network. *Journal of Manufacturing Science and Engineering*, 2021, 143, 051013.
20. Ying X. An overview of overfitting and its solutions[C]//*Journal of physics: Conference series*. IOP Publishing, 2019, 1168, 022022.
21. Liu, H.; Miao, E.; Wei, X. Y.; Zhuang, X. D. Robustness Modeling Method for Thermal Error of CNC Machine Tools Based on Ridge Regression Algorithm. *International Journal of Machine Tools & Manufacture* 2017, 113, pp. 35–48.
22. Hoerl, A. E.; Kennard, R.W. Ridge regression: Biased estimation for nonorthogonal problems. *Technometrics* 1970, 42, pp. 80–86.

Disclaimer/Publisher's Note: The statements, opinions and data contained in all publications are solely those of the individual author(s) and contributor(s) and not of MDPI and/or the editor(s). MDPI and/or the editor(s) disclaim responsibility for any injury to people or property resulting from any ideas, methods, instructions or products referred to in the content.